Inorg. Chem. **2007**, *46*, 5630–5641

Photoinduced Electron Transfer across Oligo-*p*-phenylene Bridges. Distance and Conformational Effects in Ru(II)–Rh(III) Dyads

Maria Teresa Indelli,*,† Claudio Chiorboli,‡ Lucia Flamigni,§ Luisa De Cola,|| and Franco Scandola*,†,‡,⊥

Dipartimento di Chimica, Università di Ferrara, 44100 Ferrara, Italy, ISOF-CNR (Sezione di Ferrara), 44100 Ferrara, Italy, ISOF-CNR, 40129 Bologna, Italy, Physikalisches Institut, Westfälische Wilhelms-Universität Münster, D-48149 Münster, Germany, and INSTM (UdR Ferrara), 44100 Ferrara, Italy

Received March 6, 2007

A series of rodlike ruthenium(II)–rhodium(III) polypyridine dyads based on modular oligo-*p*-phenylene bridges, of the general formula $[(Me_2phen)_2Ru–bpy–(ph)_n–bpy–Rh(Me_2bpy)]^{5+}$ (Me_2phen = 4,7-dimethyl-1,10-phenanthroline; bpy = 2,2′-bipyridine; ph = 1,4-phenylene; n = 1–3), have been synthesized and their photophysical properties investigated. The dyad $[(Me_2bpy)_2Ru–bpy–(ph)_3'–bpy–Rh(Me_2bpy)]^{5+}$ with the central phenylene unit bearing two hexyl chains has also been studied. The metal-to-metal distance reaches 24 Å for the longest (n = 3) spacer in the series. For all of the dyads in a room-temperature CH_3CN solution, quenching of the typical metal-to-ligand charge-transfer luminescence of the Ru-based chromophoric unit is observed, indicating that an efficient intramolecular photoinduced electron transfer from the excited Ru moiety to the Rh-based unit takes place. The rate constants for the electron-transfer process have been determined by time-resolved emission and absorption spectroscopy in the nanosecond and picosecond time scale. An exponential dependence of experimental transfer rates on the bridge length is observed, consistent with a superexchange mechanism. An attenuation factor β of 0.65 $Å^{-1}$ is determined, in line with the behavior of other systems containing oligo-*p*-phenylene spacers. Interestingly, for n = 3, the presence/absence of hexyl substituents in the central *p*-phenylene ring causes a 10-fold difference in the rates between otherwise identical dyads. This comparison highlights the importance of the twist angle between adjacent spacers on the overall through-bond donor–acceptor coupling.

Introduction

The design and construction of molecular-level electronic devices is a subject of considerable interest at the interface between supramolecular chemistry and nanotechnology.[1−3] The basic idea is that functions characteristic of electronic devices can be emulated by appropriate supramolecular structures, where individual molecules play the role of electronic components. As the simplest of components of a molecular electronic set, *molecular wires*[4] have attracted a great deal of attention. This term is not precisely defined, being used with different meanings by different authors and

* To whom correspondence should be addressed. E-mail: idm@unife.it (M.T.I.), snf@unife.it (F.S.).
† Università di Ferrara.
‡ ISOF-CNR (Sezione di Ferrara).
§ ISOF-CNR.
|| Westfälische Wilhelms-Universität Münster.
⊥ INSTM.

(1) (a) *Molecular Electronic Devices*; Carter, F. L., Siatkowsky, R. E., Woltjien, H., Eds.; Elsevier: Amsterdam, The Netherlands, 1988. (b) *Molecular Electronics*; Jortner, J., Ratner, M., Eds.; Blackwell: London, U.K., 1997. (c) Rouvray, D. *Chem. Br*. **1998**, *34*, 26. (d) *Molecular Electronics III*; Reimers, J. R., Picconatto, C. A., Ellenbogen, J. C., Shashidhar, R., Eds.; New York Academy of Sciences: New York, 2003.

(2) (a) Lehn, J.-M. *Angew. Chem., Int. Ed. Engl*. **1988**, *27*, 89; **1990**, *29*, 1304. (b) Lehn, J.-M. *Supramolecular Chemistry*; VCH: Weinheim, Germany, 1995. (c) *Comprehensive Supramolecular Chemistry*; Atwood, J. L., Davies, J. E. D., MacNicol, D. D., Vögtle, F., Eds.; Pergamon/Elsevier: Oxford, U.K., 1996. (d) Balzani, V.; Scandola, F. *Supramolecular Photochemistry*; Horwood: Chichester, U.K., 1991. (e) Balzani, V.; Scandola, F. In *Comprehensive Supramolecular Chemistry*; Reinhoudt, D. N., Ed.; Pergamon Press: Oxford, U.K., 1996; Vol. 10, p 687. (e) Balzani, V.; Credi, A.; Venturi, M. In *Supramolecular Science: Where We Are and Where We Are Going*; Ungaro, R., Dalcanale, E., Eds.; Kluwer: Dordrecht, The Netherlands, 1999; p 1.

(3) (a) Tour, J. M.; Kozaki, M.; Seminario, J. M. *J. Am. Chem. Soc*. **1998**, *120*, 8486. (b) Seminario, J. M.; Tour, J. M. In *Molecular Electronics—Science and Technology*; Aviran, A., Ratner, M. A., Eds.; New York Academy of Sciences: New York, 1998; p 69. (c) Tour, J. M. *Acc. Chem. Res*. **2000**, *33*, 791. (d) Tour, J. M. *Molecular Electronics: Commercial Insights, Chemistry, Devices, Architecture and Programming*; World Scientific: Hackensack, NJ, 2003.

(4) De Cola, L. Molecular Wires: From Design to Properties. *Top. Curr. Chem*. **2005**, *257*, 1.

10.1021/ic700430u CCC: $37.00
Published on Web 06/12/2007

in different contexts. In a very broad sense, however, it can be used to designate one-dimensional molecular structures that, when interposed between appropriate donor and acceptor terminal sites, efficiently mediate the transfer of electrons between those sites. Molecular wires can be studied in a variety of chemical/physical systems, depending on the nature of the donor and acceptor terminals that the wire is connected to and on the method used to detect the electron flow. Available techniques include the following: (i) photoinduced electron transfer in donor−wire−acceptor dyads,[5] (ii) fast electrochemistry on self-assembled monolayers (SAMs) of wires containing electroactive groups,[6−9] (iii) electrical measurements on metal−SAM−SAM−metal junctions based on Hg drop electrodes,[10] (iv) measurement of single-molecule conductivity within a break junction,[11] (v) probing of single molecules with scanning tunneling microscopy,[12−14] or atomic force microscope experiments.[15]

At the molecular level, the term "wire" should not be taken literally because it tends to evoke the idea of a conventional ohmic-type conductor. In fact, for many experimental cases involving saturated or partially unsaturated organic bridges, this is not the case. In such systems, the energy levels of the wires investigated are far apart from those of the donor and acceptor sites (for the lowest unoccupied molecular orbital, higher than the donor, and for the highest occupied molecular orbital, lower than the acceptor). Therefore, the electron tunnels across the wire *in a single step* from donor to acceptor, without being localized at any time on the wire. These processes are described by standard nonadiabatic electron-transfer theory,[16] where the transfer probability is proportional to the square of the donor−acceptor electronic coupling. The role of the connecting wire is actually that of a mediator of donor−acceptor electronic coupling. The phenomenon is conveniently described in terms of superexchange.[5,17] The electron-transfer probability k_{el} decreases exponentially with the donor−acceptor distance r_{DA} (eq 1), and the intrinsic properties of the wire are represented by the attenuation factor β.

$$k_{el} = k(0)\exp(-\beta r_{DA}) \quad (1)$$

In this regime, therefore, the molecular wire behaves very differently from an ohmic conductor (although terms such as "insulating" or "conducting" are sometimes still conventionally used to indicate wires with high or low β values).

In particular cases, namely with highly delocalized organic bridges, the wire levels may become accessible from the donor or acceptor sites. In such cases, the electron transfer may proceed stepwise by injection of electrons (or holes) into the wire. This type of process can be appropriately called "electron transport"[5a] and has an expected inverse dependence on a small power (1−2) of the distance, more similar to conventional ohmic conduction. In some conjugated systems, a switch in the mechanism from superexchange to injection (from electron transfer to electron transport) can occur with an increase in the length of the wire, for example, when the levels of the wire fall below the filled level of the donor.[18]

In the search for molecular wires that may have low values of β while still remaining in the superexchange regime, substantial attention has been devoted to oligo-*p*-phenylene bridges. These types of bridges are attractive because of their modular nature and longitudinal rigidity. Furthermore, they are made of individual units with delocalized π systems, but extensive delocalization is prevented because nonbonded interactions force adjacent units in a twisted geometry (ca. 40° angle in the gas phase).[19] Onuchich and Beratan[20] first considered electron transfer through biphenyl spacers from a theoretical viewpoint. In pioneering experimental work by McLendon and co-workers[21] on bis(porphyrin) systems with oligo-*p*-phenylene spacers, a 7-fold attenuation in the photoinduced electron-transfer rate was obtained for each added

(5) (a) Paddon-Row, M. N. In *Electron Transfer in Chemistry*; Balzani, V., Ed.; Wiley-VCH: Weinheim, Germany, 2001; Vol. III, Chapter 2.1, p 179. (b) Scandola, F.; Chiorboli, C.; Indelli, M. T.; Rampi, M. A. In *Electron Transfer in Chemistry*; Balzani, V., Ed.; Wiley-VCH: Weinheim, Germany, 2001; Vol. III, Chapter 2.3, p 337. (c) Petersson, K.; Wiberg, J.; Ljungdahl, T.; Martensson, J.; Albinsson, B. *J. Phys. Chem. A* **2006**, *110*, 319.

(6) Chidsey, C. E. D. *Science* **1991**, *251*, 919.

(7) Weber, K.; Creager, S. E. *Anal. Chem.* **1994**, *66*, 3164.

(8) Creager, S.; Yu, C. J.; Bamad, C.; O'Connor, S.; MacLean, T.; Lam, E.; Chong, Y.; Olsen, G. T.; Luo, J.; Gozin, M.; Kayyem, J. F. *J. Am Chem. Soc*. **1999**, *121*, 1059.

(9) (a) Sachs, S. B.; Dudek, S. P.; Hsung, R. P.; Sita, L. R.; Smalley, J. F.; Newton, M. D.; Feldberg, S. W.; Chidsey, C. E. D. *J. Am. Chem. Soc.* **1997**, *119*, 10563. (b) Sykes, H. D.; Smalley, J. F.; Dudek, S. P.; Cook, A. R.; Newton, M. D.; Chidsey, C. E. D.; Felberg, S. W. *Science* **2001**, *291*, 1519.

(10) (a) Haag, R.; Rampi, M. A.; Holmlin, R. E.; Whitesides, G. M. *J. Am. Chem. Soc.* **1999**, *121*, 7895. (b) Holmlin, E. H.; Ismagilov, R. F.; Haag, R.; Mujica, V.; Ratner, M. A.; Rampi, M. A.; Whitesides, G. M. *Angew. Chem., Int. Ed*. **2001**, *40*, 2316. (c) Tran, E.; Ferri, V.; Zharnikov, M.; Muellen, K.; Whitesides, M. G.; Rampi, M. A. *Adv. Mater*. **2006**, *18*, 1323.

(11) Reed, M. A.; Zhou, C.; Muller, C. J.; Burgin, T. P.; Tour, J. M. *Science* **1997**, *278*, 252.

(12) Donhauser, Z. J.; Mantooth, B. A.; Kelly, K. F.; Bumm, L. A.; Monnell, J. D.; Stapleton, J. J.; Price, D. W., Jr.; Rawlett, A. M.; Allara, D. L.; Tour, J. M.; Weiss, P. S. *Science* **2001**, *292*, 2303.

(13) Andreas, R. P.; Bein, T.; Dorogi, M.; Feng, S.; Henderson, J. I.; Kubiak, C. P.; Mahoney, W.; Osifchin, R. G.; Reifenberger, R. *Science* **1996**, *272*, 1323.

(14) (a) Xu, B.; Tao, N. J. *Science* **2003**, *301*, 1221. (b) He, J.; Chen, F.; Li, J.; Sankey, O. F.; Terazono, Y.; Herrero, C.; Gust, D.; Moore, T. A.; Moore, A. L.; Lindsay, S. M. *J. Am. Chem. Soc*. **2005**, *127*, 1384.

(15) (a) Leathermann, G.; Durantini, E. N.; Gust, D.; Moore, T. A.; Moore, A. L.; Stone, S.; Zhou, Z.; Rez, P.; Liu, Y. Z.; Lindsay, S. M. *J. Phys. Chem. B* **1999**, *103*, 4006. (b) Ramachandran, G. K.; Tomfohr, J. K.; Li, J.; Sankey, O. F.; Zarate, X.; Primak, A.; Terazano, Y.; Moore, T. A.; Moore, A. L.; Gust, D.; Nagahara, L. A.; Lindsay, S. M. *J. Phys. Chem. B* **2003**, *107*, 6162. (c) Cui, X. D.; Primak, A.; Zarate, X.; Tomfohr, J.; Sankey, O. F.; Moore, A. L.; Moore, T. A.; Gust, D.; Harris, G.; Lindsay, S. M. *Science* **2001**, *294*, 571.

(16) (a) Marcus, R. A. *Annu. Rev. Phys. Chem*. **1964**, *15*, 155. (b) Sutin, N. *Prog. Inorg. Chem*. **1983**, *30*, 441. (c) Miller, J. R.; Beitz, J. V.; Huddleston, R. K. *J. Am. Chem. Soc.* **1984**, *106*, 5057. (d) Marcus, R. A.; Sutin, N. *Biochim. Biophys. Acta* **1985**, *811*, 265. (e) Jortner, J. *J. Chem. Phys.* **1976**, *64*, 4860. (f) Bixon, M.; Jortner, J. *Adv. Chem. Phys.* **1999**, *106*, 35. (g) Newton, M. D. *Chem. Rev.* **1991**, *91*, 767.

(17) (a) Halpern, J.; Orgel, L. E. *Discuss. Faraday Soc.* **1960**, *29*, 32. (b) McConnell, H. M. *J. Chem. Phys.* **1961**, *35*, 508. (c) Mayoh, B.; Day, P. *J. Chem. Soc., Dalton Trans.* **1974**, 846. (d) Miller, J. R.; Beitz, J. V. *J. Chem. Phys.* **1981**, *74*, 6746. (e) Richardson, D. E.; Taube, H. *J. Am. Chem. Soc.* **1983**, *105*, 40.

(18) Davis, W. B.; Svec, W. A.; Ratner, M. A.; Wasielewski, M. R. *Nature* **1998**, *396*, 60.

(19) Zojer, E.; Cornil, J.; Leising, G.; Brédas, J. L. *Phys. Rev. B* **1999**, *59*, 7957.

(20) Onuchic, J. N.; Beratan, D. N. *J. Am. Chem. Soc*. **1987**, *109*, 6771.

(21) (a) Helms, A.; Heiler, D.; McLendon, G. *J. Am. Chem. Soc.* **1991**, *113*, 4325. (b) Helms, A.; Heiler, D.; McLendon, G. *J. Am. Chem. Soc.* **1992**, *114*, 6227.

additional *p*-phenylene unit ($\beta = 0.4$ Å^{-1}).[21b] Extensive work has recently been performed by Wasielewski and co-workers on oligo-*p*-phenylene-bridged dyads, where perylenebis(imide) acts as a photoexcited acceptor and phenothiazine as the electron donor quencher.[22] Subsequently, extensive series of inorganic dyads with ruthenium(II) and osmium(II) polypyridyl complexes as donor and acceptor units and oligo-*p*-phenylene spacers were investigated by Sauvage and co-workers[23] and by De Cola and co-workers.[24] Such dyads, however, were suitable for the study of triplet *energy* transfer rather than electron transfer. In the most extensive study, involving up to five phenylene spacers, the experimental distance dependence of the energy-transfer rates corresponded to $\beta = 0.50$ Å^{-1}.[24c] Recently, another series of oligo-*p*-phenylene-bridged complexes containing iridium(III) and ruthenium(II) polypyridine units has been studied, where intercomponent energy transfer shows a very weak distance dependence ($\beta = 0.07$ Å^{-1}), consistent with a hopping-type mechanism.[25]

We have now synthesized the series of ruthenium(II)−rhodium(III) polypyridine dyads shown in Chart 1. Given their excited-state energies and redox potentials (vide infra), these dyads lend themselves to the study of photoinduced electron transfer from the Ru(II) to the Rh(III) component. Different from previously studied analogues based on terpyridine ligands,[26] the Ru(II) molecular component has an intrinsically long excited-state lifetime and is thus a good potential donor for long-range electron transfer. The series of compounds **Ru**−**ph**$_n$−**Rh** ($n = 1-3$) is suitable for the investigation of the distance dependence of electron transfer.[27] In the **Ru**−**ph**$_3$′−**Rh** complex, the hexyl substituents on the central *p*-phenylene spacer were originally introduced for solubility and synthetic ease. Comparison with the unsubstituted **Ru**−**ph**$_3$−**Rh** complex, however, may yield information on the torsional effects of the behavior of such molecular wires.[28]

Chart 1

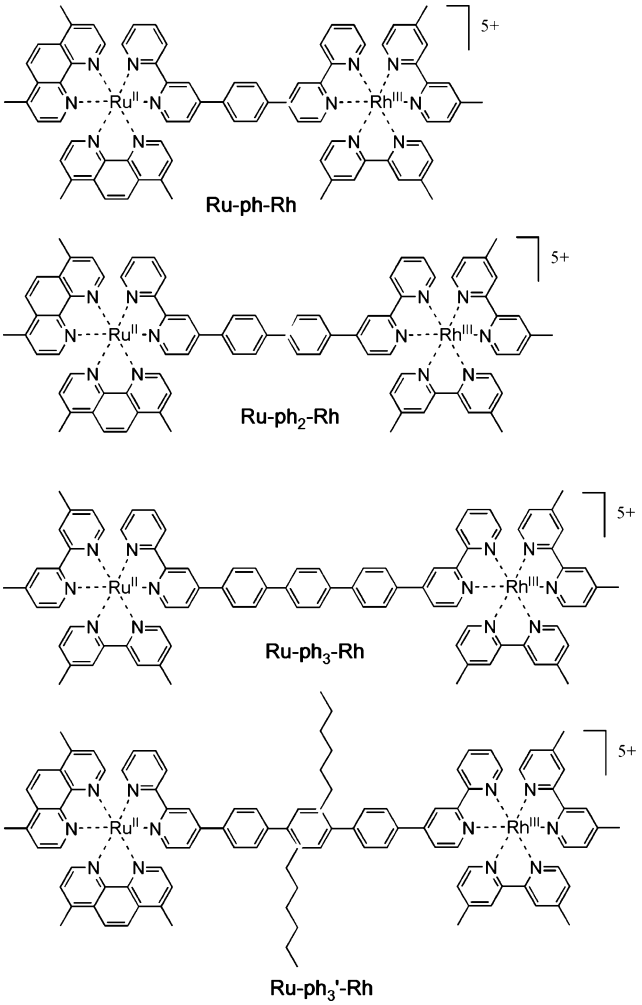

Experimental Section

Materials. $(NH_4)_3RhCl_6$, $RuCl_3 \cdot 3H_2O$, 4,4′-dimethyl-2,2′-bipyridine (Me_2bpy), 4,7-dimethyl-1,10-phenanthroline (Me_2phen), tetrakis(triphenylphosphine)palladium(0) (Aldrich), and 4,4′-phenyldiboronic acid (Lancaster) were commercial products and were used as received.

For photophysical measurements, spectrograde organic solvents (Merk Uvasol) were used without further purification. Other chemicals were all of reagent-grade quality.

The precursor complexes $Ru(Me_2phen)_2Cl_2$,[29] $Ru(Me_2bpy)_2Cl_2$,[29] $[Ru(Me_2bpy)_2(bpy-ph-Br)](PF_6)_2$,[30] $[Rh(Me_2bpy)_2Cl_2]Cl$,[31] and $[Rh(Me_2bpy)_2(bpy-ph-Br)](PF_6)_3$[30] were prepared according to literature procedures. $[Rh(Me_2bpy)_3](PF_6)_3$, $[Ru(Me_2phen)_3](PF_6)_2$, and $[Ru(Me_2bpy)_3](PF_6)_2$ were available from previous work.[31]

Sephadex CM-C25 (Pharmacia) was used in ionic exchange chromatography. Silica gel (Merck) used in chromatographic purification was 200−400 mesh. Preparative thick-layer chromatography was performed on Analtech silica gel G uniplates (soft layer, 20 × 20 cm, 1000 μm).

(22) (a) Weiss, E. A.; Ahrens, M. J.; Sinks, L. E.; Ratner, M. A.; Wasielewski, M. R. *J. Am. Chem. Soc.* **2004**, *126*, 5577. (b) Weiss, E. A.; Ahrens, M. J.; Sinks, L. E.; Ratner, M. A.; Wasielewski, M. A. *J. Am. Chem. Soc.* **2004**, *126*, 9510. (c) Weiss, E. A.; Tauber, M. J.; Kelley, R. F.; Ahrens, M. J.; Ratner, M. A.; Wasielewski, M. R. *J. Am. Chem. Soc.* **2005**, *127*, 11842.

(23) (a) Barigelletti, F.; Flamigni, L.; Guardigli, M.; Juris, A.; Beley, M.; Chodorowski-Kimmes, S.; Collin, J.-P.; Sauvage, J.-P. *Inorg. Chem.* **1996**, *35*, 136. (b) Barigelletti, F.; Flamigni, L.; Collin, J.-P.; Sauvage, J.-P. *Chem. Commun.* **1997**, 333. (c) Collin, J.-P.; Gavina, P.; Heitz, V.; Sauvage, J.-P. *Eur. J. Inorg. Chem.* **1998**, 1.

(24) (a) Schlicke, B.; Belser, P.; De Cola, L.; Sabbioni, E.; Balzani, B. *J. Am. Chem. Soc.* **1999**, *121*, 4207. (b) De Cola, L.; Belser, P. In *Electron Transfer in Chemistry*; Balzani, V., Ed.; Wiley-VCH Verlag GmbH: Weinheim, Germany, 2001; Vol. 5, p 97. (c) Welter, S.; Salluce, N.; Belser, P.; Groeneveld, M.; De Cola, L. *Coord. Chem. Rev.* **2005**, *249*, 1360.

(25) Welter, S.; Lafolet, F.; Cecchetto, E.; Vergeer, F.; De Cola, L. *Chem. Phys. Chem.* **2005**, *6*, 2417.

(26) (a) Indelli, M. T.; Scandola, F.; Collin, J.-P.; Sauvage, J.-P.; Sour, A. *Inorg. Chem.* **1996**, *35*, 303. (b) Indelli, M. T.; Scandola, F.; Flamigni, L.; Collin, J.-P.; Sauvage, J.-P.; Sour, A. *Inorg. Chem.* **1997**, *36*, 4247.

(27) For practical reasons, in the dyad **Ru**−**ph**$_3$−**Rh** at the Ru center, the terminal phenanthroline ligands are replaced by bipyridine-type ligands. For $Ru(4,4'\text{-}Me_2bpy)_3^{2+}$ and $Ru(4,7\text{-}Me_2phen)_3^{2+}$ homoleptic complexes, the redox potentials and the MLCT energy values are very similar; thus, the two chromophores, $Ru(4,4'\text{-}Me_2bpy)_2(bpy)^{2+}$ and $Ru(4,7\text{-}Me_2phen)_2(bpy)^{2+}$, can be considered to be identical from a photophysical point of view.

(28) A preliminary account of this work has been included in a review article: Chiorboli, C.; Indelli, M. T.; Scandola, F. *Top. Curr. Chem.* **2005**, *257*, 63.

(29) Sullivan, B. P.; Salomon, D. J. *J. Inorg. Chem.* **1978**, *17*, 3334.

(30) Bossart, O.; De Cola, L.; Welter, S.; Calzaferri, G. *Chem.—Eur. J.* **2004**, *10*, 5771.

(31) Indelli, M. T.; Bignozzi, C. A.; Harriman, A.; Schoonover, J. R.; Scandola, F. *J. Am. Chem. Soc.* **1994**, *116*, 3768.

Chart 2

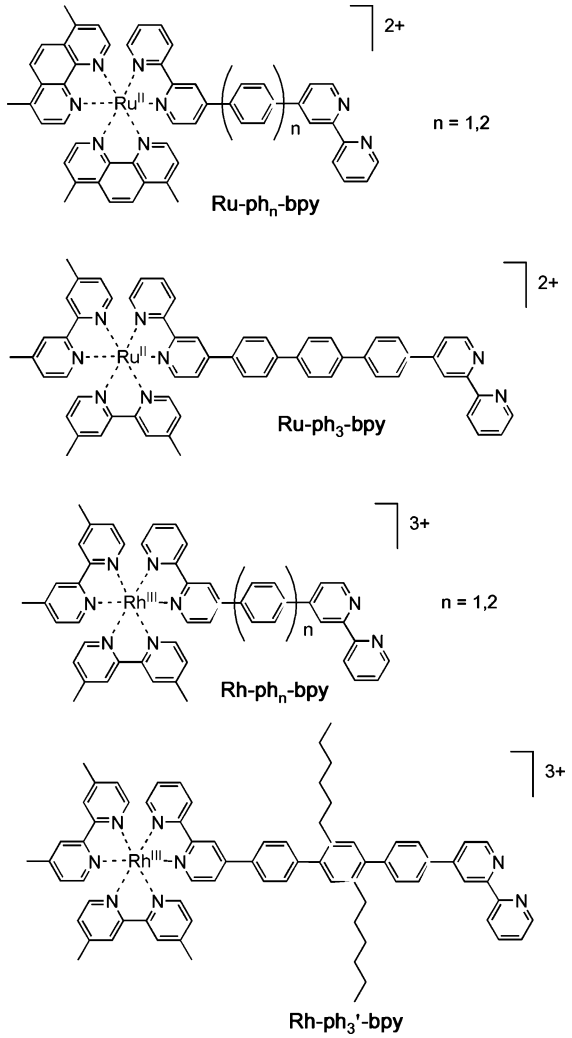

Syntheses. (i) Ligands. 4-(4′-Bromophenyl)-2,2′-bipyridine (bpy−ph−Br) ligand and the bridging ligands bpy−ph−bpy and bpy−ph_2−bpy were prepared by the method described by Schmehl and co-workers.[32] The bpy−ph_3′−bpy ligand was available from a previous work.[24a]

(ii) Mononuclear Complexes. A number of mononuclear Ru(II) and Rh(III) complexes (Chart 2) are used in this work as model compounds. All of the complexes were isolated as PF_6^- salts. The complexes were identified by ^{1}H NMR and mass spectroscopy (electron spray ionization, ESI-MS).

The Ru model complexes **Ru−ph−bpy** and **Ru−ph_2−bpy** were prepared by following the method published for the analogous [Ru(Me_2phen)$_2$(Mebpy−CH_2−CH_2Mebpy)]$(PF_6)_2$,[31] starting from Ru(Me_2phen)$_2Cl_2$ and using the appropriate bridging ligand. The synthesis of **Ru−ph_3−bpy** is reported elsewhere.[30]

The syntheses of the Rh mononuclear complexes, **Rh−ph−bpy**, **Rh−ph_2−bpy**, and **Rh−ph_3′−bpy**, were carried out starting from [Rh(Me_2bpy)$_2Cl_2$]Cl as the precursor with a 2-fold excess of the appropriate bridging ligand to minimize the formation of binuclear species. The same general procedure was followed for all three complexes with minor changes concerning the reaction time and the solvent reaction mixture. A typical synthesis is described below for **Rh−ph_2−bpy**.

(32) (a) Baba, A. I.; Schmell, R. *Synth. Commun.* **1994**, *24*, 1029. (b) Baba, A. I.; Ensley, H. E.; Schmell, R. *Inorg. Chem*. **1995**, *34*, 1198.

[Rh(Me_2bpy)$_2$(bpy−ph_2−bpy)]$(PF_6)_3$. A 116-mg (0.25 mmol) amount of bpy−ph_2−bpy was dissolved in 80 mL of a hot 40/60 ethylene glycol/ethanol solution. To this solution was added dropwise (0.1 mL/min), under continuous stirring at 90 °C to avoid precipitation of the bpy−ph_2−bpy ligand, 73 mg (0.125 mmol) of [Rh(Me_2bpy)$_2Cl_2$]Cl, separately dissolved in 15 mL of 1/1 ethanol/water. The reaction mixture was then refluxed for 72 h. After evaporation of ethanol, the solution was allowed to cool to room temperature, diluted to 300 mL with water, and filtered to remove the excess of the bridging ligand. The filtrate solution containing the desired product as Cl^- salt was purified by cationic exchange chromatographic loading onto a CM-C25 Sephadex column in Na^+ form and using NaCl as the eluent. Some unreacted [Rh(Me_2bpy)$_2Cl_2$]$^+$ was first eluted with 0.05 M NaCl; then the product was collected with 0.5 M NaCl. This fraction was concentrated and the pure product precipitated by the addition of $NaPF_6$. The solid was isolated by filtration, washed extensively with water, and dried under vacuum. Yield: 65%. ^{1}H NMR and mass spectral data (ESI) are given below for each Rh complex.

(a) [Rh(Me_2bpy)$_2$(bpy−ph−bpy)]$(PF_6)_3$. ^{1}H NMR (400 MHz, CD_3CN): δ 8.97 (d, 1H, J = 1.9 Hz), 8.90 (d, 1H, J = 8.2 Hz), 8.85 (d, 1H, J = 5.5 Hz), 8.83 (d, 1H, J = 1.2 Hz), 8.78 (d, 1H, J = 4.7 Hz), 8.60−8.47 (m, 6H), 8.18−8.10 (m, 5H), 8.00 (dd, 1H, J = 6.2 and 2.1 Hz), 7.92 (dd, 1H, J = 5.3 and 1.7 Hz), 7.79−7.72 (m, 3H), 7.66−7.52 (m, 9H), 2.68 (s, 1CH_3), 2.67 (s, 1CH_3), 2.66 (s, 2CH_3). MS (ESI): m/z 286.0 ([M − 3PF_6]$^{3+}$/3 requires m/z 286.0), 501.3 ([M − 2PF_6]$^{2+}$/2 requires m/z 501.3).

(b) [Rh(Me_2bpy)$_2$(bpy−ph_2−bpy)]$(PF_6)_3$. ^{1}H NMR (400 MHz, CD_3CN): δ 8.98 (m, 1H), 8.92 (m, 1H), 8.80 (m, 1H), 8.72 (m, 1H), 8.57 (m, 4H), 8.50 (m, 2H) 8.14−7.90 (m, 11H), 7.80−7.70 (m, 4H), 7.64 (m, 1H), 7.60−7.48 (m, 8H), 2,68 (s, 1CH_3), 2.66 (bs, 3CH_3). MS (ESI): m/z 311.4 ([M − 3PF_6]$^{3+}$/3 requires m/z 311.2), 539.3 ([M − 2PF_6]$^{2+}$/2 requires m/z 593.3).

(c) [Rh(Me_2bpy)$_2$(bpy−ph_3′−bpy)]$(PF_6)_3$. ^{1}H NMR (400 MHz, CD_3CN): δ 8.97 (m, 1H), 8.90 (d, 1H, J = 8.2 Hz), 8.81−8.72 (m, 3H), 8.60−8.48 (m, 6H), 8.10−7.93 (m, 6H), 7.80−7.62 (m, 8H), 7.60−7.50 (m, 8H), 7.46 (m, 1H), 7.28 (s, 1H), 7.24 (s, 1H), 2.68 (m, 4CH_3 + 2CH_2), 1.60−0.78 (m, 22H). MS (ESI): m/z 392.6 ([M − 3PF_6]$^{3+}$/3 requires m/z 392.8), 661.4 ([M − 2PF_6]$^{2+}$/2 requires m/z 661.6).

(iii) Dyads. (a) [(Me_2phen)$_2$Ru(bpy−ph−bpy)Rh(Me_2bpy)$_2$]$(PF_6)_5$ (Ru−ph−Rh). [Rh(Me_2bpy)$_2$(bpy−ph−bpy)]$(PF_6)_3$ (94 mg, 0.092 mmol) was dissolved in methanol (30 mL) with 5% dimethylformamide (DMF) content. After the addition of Ru(Me_2phen)$_2Cl_2$ (46 mg, 0.080 mmol), the solution was refluxed for 20 h under argon. The solvent was evaporated, and acetonitrile (10 mL) and NH_4PF_6 (50 mg) were added. The PF_6^- salt was precipitated by the addition of water (100 mL) and evaporation of acetonitrile and collected by filtration. The precipitate was washed extensively with water and air-dried. The crude product was dissolved in a minimum of acetonitrile and purified from unreacted [Rh(Me_2bpy)$_2$(bpy−ph−bpy)]$(PF_6)_3$ on a silica gel column with 40/10/10/1 MeCN/MeOH/H_2O/saturated aqueous KNO_3 as the eluent. An orange compound was isolated as the main fraction and further purified by preparative thick-layer chromatography [SiO_2, 40/10/1 (v/v) MeCN/H_2O/saturated aqueous KNO_3 as the mobile phase). Recrystallization from acetonitrile/water yielded an orange-red solid. Yield: 30%.^{1}H NMR (400 MHz, CD_3CN): δ 8.76 (m, 1H), 8.90 (m, 1H), 8.84 (m, 1H), 8.75 (m, 1H), 8.56 (m, 5H), 8.42 (m, 4H), 8.18−8.10 (m, 4H), 7.80−7.50 (m, 22H), 7.44 (m, 2H), 7.52 (m, 1H), 2.97 (s, 2CH_3), 2.89 (s, 2CH_3), 2.67 (bs, 4CH_3); MS (ESI): m/z 380.2 ([M − 4PF_6]$^{4+}$/4 requires m/z 380.2), 555.1 ([M − 3PF_6]$^{3+}$/3 requires m/z 555.2).

(b) [(Me_2phen)$_2$Ru(bpy−ph$_2$−bpy)Rh(Me_2bpy)$_2$](PF$_6$)$_5$ (Ru−ph$_2$−Rh). This compound was prepared as described for **Ru−ph−Rh** starting from the appropriate Rh precursor, [Rh(Me_2bpy)$_2$(bpy−ph$_2$−bpy)](PF$_6$)$_3$. Yield: 25%. ^{1}H NMR (400 MHz, CD_3CN): δ 9.00−8.88 (m, 2H), 8.83 (m, 1H), 8.75 (m, 1H), 8.56 (m, 5H), 8.42 (m, 4H), 8.14−7.96 (m, 8H), 7.80−7.48 (m, 22H), 7.44 (m, 2H), 7.30 (m, 1H), 2.97 (s, 2CH_3), 2.89 (s, 2CH_3), 2.67 (bs, 4CH_3). MS (ESI): *m*/*z* 290.5 ([M − 5PF$_6$]$^{5+}$/5 requires *m*/*z* 290.4).

(c) [(Me_2phen)$_2$Ru(bpy−ph$_3$′−bpy)Rh(Me_2bpy)$_2$](PF$_6$)$_5$ (Ru−ph$_3$′−Rh). This compound was prepared as described for **Ru−ph−Rh** starting from the appropriate Rh precursor, [Rh(Me_2bpy)$_2$(bpy−ph$_3$′−bpy)](PF$_6$)$_3$. Yield: 30%. ^{1}H NMR (400 MHz, CD_3CN): δ 8.96 (bs, 1H), 8.90 (d, 1H, J = 8.6 Hz), 8.84 (bs, 1H), 8.74 (d, 1H, J = 8.4 Hz), 8.56 (d, 5H, J = 6.0 Hz), 8.42 (m, 3H), 8.16−8.04 (m, 5H) 8.03−7.94 (m, 3H), 7.80−7.50 (m, 24H), 7.44 (m, 2H), 7.24 (s, 2H), 2.98 (s, 2CH_3), 2.89 (s, 2CH_3), 2.65 (bs, 4CH_3 + 2CH_2), 1.60−0.70 (m, 22H). MS (ESI): *m*/*z* 339.4 ([M − 5PF$_6$]$^{5+}$/5 requires *m*/*z* 339.2).

(d) [(Me_2bpy)$_2$Ru(bpy−ph$_3$−bpy)Rh(Me_2bpy)$_2$](PF$_6$)$_5$ (Ru−ph$_3$−Rh). This dyad was prepared in a single step by a Suzuki cross-coupling reaction following the method described by De Cola and co-workers for the synthesis of analogous polyphenylene-bridged bimetallic Ru complexes.[33] The starting compounds are [Ru(Me_2bpy)$_2$(bpy−ph−Br)](PF$_6$)$_2$ and [Rh(Me_2bpy)$_2$(bpy−ph−Br)](PF$_6$)$_3$, both containing one functionalized 4-(4′-bromophenyl)-2,2′-bipyridine ligand. The cross-coupling reaction with 1,4-benzenediboronic acid, using Pd(0) as a catalyst, yields the Ru−Rh dyad containing three phenylene units as spacers. In a typical synthesis, [Ru(Me_2bpy)$_2$(bpy−ph−Br)](PF$_6$)$_2$ (30 mg, 0.028 mmol), [Rh(Me_2bpy)$_2$(bpy−ph−Br)](PF$_6$)$_3$ (40 mg, 0.034 mmol), 4,4′-phenyldiboronic acid (6 mg, 0.034 mmol), and K_2CO_3 (45 mg, 0.34 mmol) were dissolved in DMF (15 mL). Pd(PPh$_3$)$_4$ (5 mg, 0.004 mmol) was added to the degassed solution, and the reaction mixture was heated to 95 °C under an argon atmosphere. After 20 h, the solvent was removed under vacuum (100 °C). The residue was washed with methanol and extensively with water and then dissolved in a minimum of acetonitrile and chromatographically loaded onto a SiO_2 column using 40/10/10/1 MeCN/MeOH/H_2O/saturated aqueous KNO_3 as the eluent. The first fractions containing the unreacted mononuclear complexes and the binuclear homometallic [Ru−ph$_3$−Ru]$^{4+}$ species were discharged. Then, the elution was continued to collect an orange fraction, which was observed to contain the desired product. This fraction was concentrated, and solid NH_4PF_6 was added. The product was precipitated as a PF_6^- salt by the addition of water and evaporation of acetonitrile and collected by filtration. This resulting product was further purified by preparative thick-layer chromatography (SiO_2, 40/10/1 (v/v) MeCN/H_2O/saturated aqueous KNO_3 as the mobile phase). Recrystallization from acetonitrile/water yielded an orange-red solid. Yield: 10%. ^{1}H NMR (400 MHz, CD_3CN): δ 8.97 (d, 1H, J = 1.8 Hz), 8.91 (d, 1H, J = 8.0 Hz), 8.80 (d, 1H, J = 1.8 Hz), 8.71 (d, 1H, J = 8.0 Hz), 8.56 (d, 4H, J = 6.5 Hz), 8.50 (m, 1H), 8.38 (d, 4H, J = 5.6 Hz), 7.94−8.14 (m, 14H), 7.82−7.70 (m, 6H), 7.66−7.52 (m, 12H), 7.44 (m, 1H), 7.28−7.22 (m, 4H), 2.68 (s, 1CH_3), 2.67 (s, 1CH_3), 2.66 (s, 2CH_3), 2.58 (s, 1CH_3), 2.56 (s, 1CH_3), 2.55 (s, 2CH_3). MS (ESI): *m*/*z* 296.3 ([M − 5PF$_6$]$^{5+}$/5 requires *m*/*z* 295.6), 406.3 ([M − 4PF$_6$]$^{4+}$/4 requires *m*/*z* 405.8).

Apparatus and Procedures. ^{1}H NMR spectra were recorded in CD_3Cl on a Varian Mercury spectrometer (400 MHz) with a residual nondeuterated solvent signal as the reference. ESI-MS spectra were measured with a Micromass ZMD2000 spectrometer.

UV−vis spectra were recorded with a Perkin-Elmer LAMDA40 spectrophotometer. Luminescence spectra were taken on a Spex Fluoromax-2 equipped with Hamamatsu R928 tubes or on a Perkin-Elmer MPF 44E spectrofluorimeter (77 K measurements). Nanosecond emission lifetimes were measured by time-correlated single-photon-counting techniques, using a PRA 3000 fluorescence spectrometer equipped with a hydrogen discharge pulsing lamp (50 kHz, half-width 2 ns), a model 1551 cooled photomultiplier, and a Norland model 5000 MCA card. The decays were analyzed by means of Edinburgh FLA 900 software (estimated error on the lifetime = ±0.1 ns). Emission lifetimes shorter than 1 ns were measured by an apparatus based on a 35-ps pulse Nd:YAG laser (PY62-10 by Continuum), with an excitation wavelength of 532 nm, and a streak camera (Hamamatsu C1587 equipped with an M1952 fast single-sweep unit). This apparatus and the procedures used to obtain the lifetimes were described in a previous paper.[26b] Nanosecond flash photolysis transient absorption experiments were performed with a Continuum Surelite Nd:YAG laser as the excitation source by using an apparatus previously described.[34] Ultrafast transient absorption measurements were performed using a pump−probe setup previously described.[35]

Cyclic voltammetric measurements were carried out with a PC-interfaced Eco Chemie Autolab/Pgstat30 potentiostat. Argon-purged solutions in CH_2Cl_2 and CH_3CN (Romil, Hi-dry) containing 0.1 M $TBAPF_6$ (Fluka; electrochemical grade, dried in an oven) were used. A conventional three-electrode cell assembly was used. A saturated calomel electrode (SCE; 6 mm^2, AMEL) and a Pt wire were used as the reference and counter electrodes, respectively; a glassy carbon electrode (8 mm^2, AMEL) was used as the working electrode. The scan rate was 200 mV/s.

Results

Synthesis of the Complexes. The dyads **Ru−ph−Rh**, **Ru−ph$_2$−Rh**, and **Ru−ph$_3$′−Rh** were prepared by the general method given in Scheme 1.

This procedure consists of the separate preparation of the bridging ligand and the mononuclear metal complex precursors. The Rh complexes [(Me_2bpy)$_2$Rh(bpy)(ph)$_n$(bpy)]$^{3+}$ (n = 1−3′) bearing a free bipyridine site were obtained by reacting the [Rh(Me_2bpy)$_2$Cl$_2$]$^+$ complex with the appropriate bridging ligand in a large excess to avoid the formation of the undesired homodinuclear Rh species (step a). The synthetic difficulties of this key step are related to the poor solubility of the bridging ligands. For the bpy−ph$_3$′−bpy bridging ligand, the solubility problem has been overcome by appending alkyl chains on the central phenylene unit. The [(Me_2phen)$_2$Rh(bpy)(ph)$_n$(bpy)]$^{3+}$ complexes are allowed to react with Ru(Me_2phen)$_2$Cl$_2$ in refluxing methanol for 10 h (step b). In all of the cases, after silica chromatography, the heterodinuclear complexes have been isolated.

The dyad **Ru−ph$_3$−Rh** has been prepared in a different way because of the insolubility of the bpy−ph$_3$−bpy bridging ligand. The synthetic strategy (Scheme 2) is based on a direct

(33) Welter, S.; Salluce, N.; Benetti, A.; Rot, N.; Belser, P.; Sonar, P.; Grimsdale, A. C.; Müllen, K.; Lutz, M.; Spek, A. L.; De Cola, L. *Inorg. Chem.* **2005**, *44*, 4706.

(34) Kleverlaan, C. J.; Indelli, M. T.; Bignozzi, C. A.; Pavanin, L.; Scandola, F.; Hasselman, G. M.; Meyer, T. J. *J. Am. Chem. Soc.* **2002**, *122*, 2840.

(35) Chiorboli, C.; Rodgers, M. A. G.; Scandola, F. *J. Am. Chem. Soc.* **2003**, *125*, 483.

Scheme 1

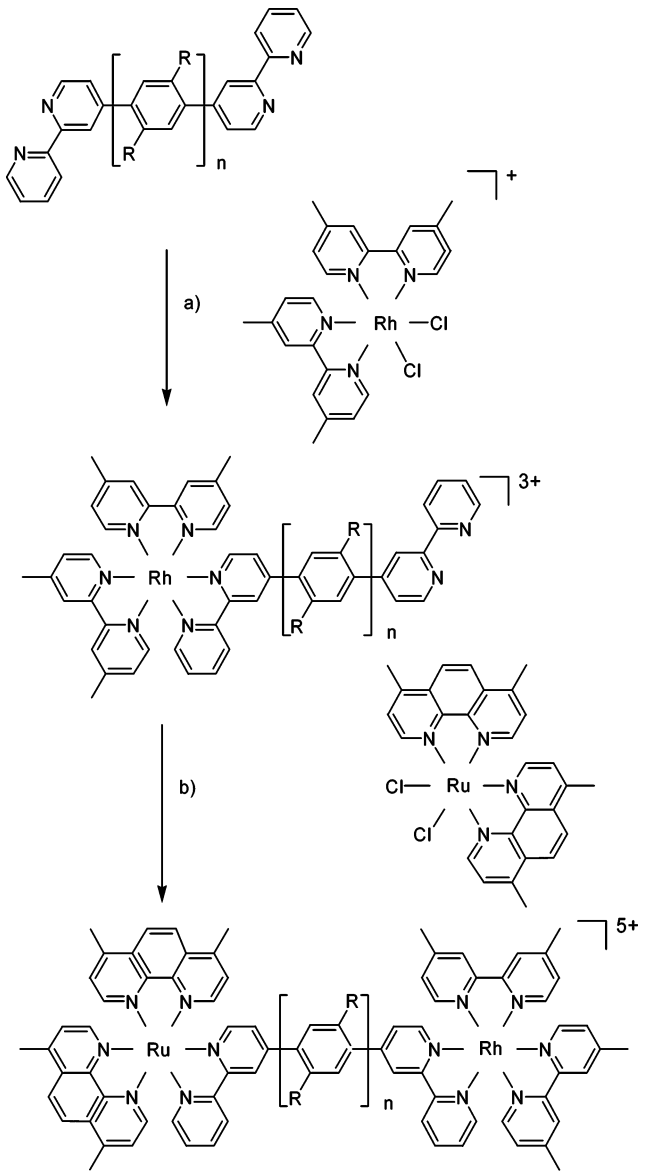

coupling of two different metal complexes by a Pd-mediated Suzuki cross-coupling reaction.[36]

The coupling process, involving a symmetric boronic acid and aryl halide derivatives of the two metal complexes, directly connects Ru and Rh centers, leading to the heterometallic dyad in one step. The homodinuclear species $[Ru-ph_3-Ru]^{4+}$ and $[Rh-ph_3-Rh]^{6+}$ formed in statistical proportion were eliminated by chromatographic purification.

Absorption Spectra. The UV−vis absorption spectra of the heterometallic **Ru−ph$_n$−Rh** dyads in an acetonitrile solution are shown in Figure 1. For the purpose of comparison, the spectra of the Rh(III) and Ru(II) mononuclear complexes (Chart 2) are also reported in parts b and c of Figure 1, respectively. These mononuclear complexes are

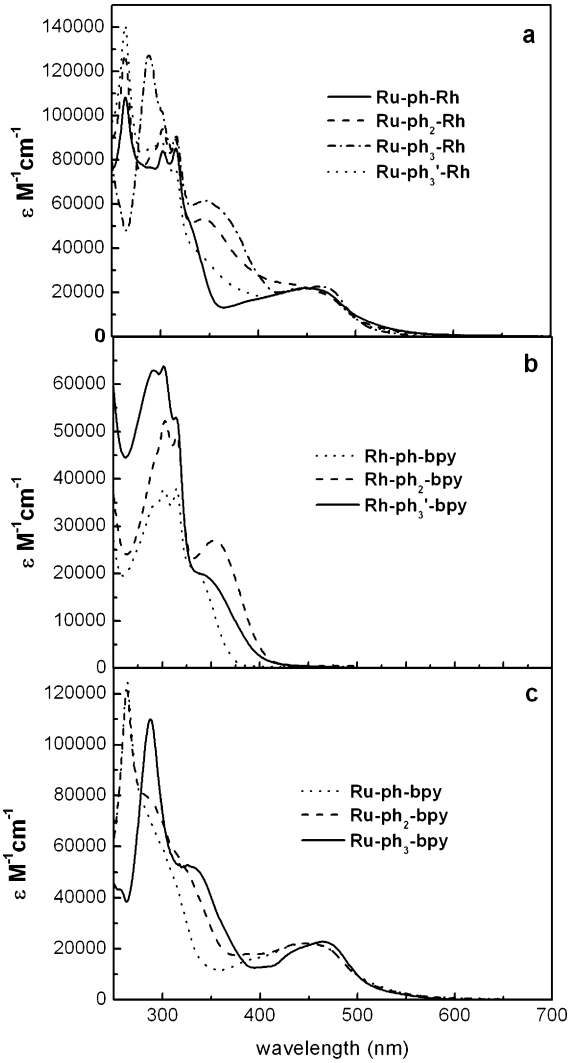

Figure 1. Absorption spectra in an acetonitrile solution at room temperature of (a) dyads **Ru−ph−Rh**, **Ru−ph$_2$−Rh**, **Ru−ph$_3$−Rh**, and **Ru−ph$_3$′−Rh**, (b) Rh model compounds **Rh−ph−bpy**, **Rh−ph$_2$−bpy**, and **Rh−ph$_3$′−bpy**, and (c) Ru model compounds **Ru−ph−bpy**, **Ru−ph$_2$−bpy**, and **Ru−ph$_3$−bpy**.

used as model compounds for the donor and acceptor units of the dyads (see the Discussion section).

The Rh(III) complexes do not absorb in the visible, whereas in the UV region, they exhibit typical ligand-centered (LC) transitions (Figure 1b). The bands at 280−320 nm are assigned to LC transitions localized on the Me$_2$bpy ligands, whereas the less-intense band at 320−400 nm (increasing in intensity and shifting by changing the number of phenylene spacers; see the Discussion section) corresponds to LC transitions of the bpy−ph$_n$−bpy bridging ligand.

The absorption spectra of the Ru(II) complexes (Figure 1c) are characterized by prominent metal-to-ligand charge-transfer transitions (MLCT) in the visible region. In this broad-band system, the overlapping contributions from two types of ligands cannot be distinguished, although the expectation is that the MLCT transition involving the bpy−ph$_n$−bpy ligand should be at a slightly lower energy than those involving Me$_2$phen and Me$_2$bpy ligands. In the UV region at 260−300 nm, the typical LC bands of the phenanthroline- and/or bipyridine-coordinated ligands are

(36) Miyara, N.; Suzuki, A. *Chem. Rev.* **1995**, *95*, 2457.

Scheme 2

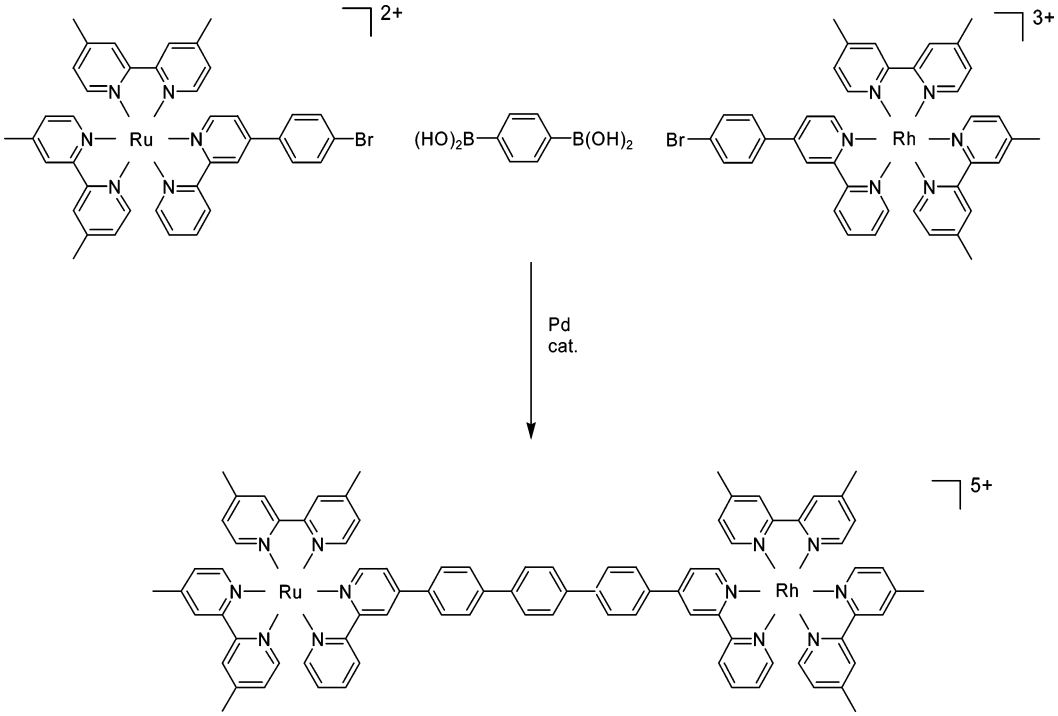

observed, whereas the LC transitions of the bpy−ph$_n$−bpy bridging ligand (increasing in intensity and shifting by changing the number and nature of phenylene spacers; see the Discussion section) appear at 300−400 nm as a shoulder of the higher energy bands.

The absorption spectra of the dyads (Figure 1a) are an approximate superposition of those of the mononuclear models. The visible region is characterized by the MLCT transitions of the Ru(II) component, without any appreciable change with respect to the model compounds. The 260−320-nm UV region is dominated by the LC transitions of both metal complex units, with distinct features of the Rh(III) component at 330 and 315 nm.[37] The 320−400-nm region is characterized by LC transitions of the bpy−ph$_n$−bpy bridging ligand, sensitive to the number and nature of phenylene spacers (see the Discussion section).

Electrochemical Behavior. The electrochemical behavior of **Ru−ph$_n$−Rh** dyads was studied by cyclic voltammetry in an acetonitrile solution (0.1 M $TBAPF_6$ supporting electrolyte, glassy carbon working electrode, SCE reference electrode, and Pt wire counter electrode). For purposes of comparison, the electrochemical behavior of the mononuclear model compounds containing one phenyl group was studied under the same experimental conditions. The results are gathered in Table 1.

The cyclic voltammetry of the Ru(II) model is typical of ruthenium(II) polypyridine complexes. The anodic region (0.0 to +1.5 V vs SCE) is characterized by a reversible oxidation wave, corresponding to oxidation of the Ru(II) center. In the cathodic region (0.0 to −1.7 V vs SCE), reversible reduction waves corresponding to one-electron reduction of the ligands are observed. The first potential is less negative than that for the homoleptic $Ru(Me_2phen)_3^{2+}$ or $Ru(Me_2bpy)_3^{2+}$, indicating that the first reduction takes place at the bpy−ph$_n$−bpy ligand.

Table 1. Redox Potentials of the **Ru−ph$_n$−Rh** Dyads and of the Model Compounds[a]

	redox process (V)			
complex	Ru(III)/Ru(II)	Rh(III)/Rh(II)	L/L$^-$(1)	L/L$^-$(2)
Rh−ph−bpy		−0.83[b]		
Ru−ph−bpy	+1.19		−1.37	−1.54
Ru−ph$_3$−bpy	+1.13		−1.34	−1.53
$[Ru(Me_2phen)_3]^{3+}$	+1.14		−1.45	−1.60
$[Ru(Me_2bpy)_3^{3+}$	+1.13		−1.45	−1.62
Ru−ph−Rh	+1.18	−0.79[b]	−1.37	−1.54
Ru−ph$_2$−Rh	+1.19	−0.84[b]	−1.31	−1.62
Ru−ph$_3$−Rh	+1.18	−0.81[b]	−1.31	
Ru−ph$_3$′−Rh	+1.18	−0.83[b]	−1.40	

[a] Cyclic voltammetry in a CH_3CN solution, 0.1 M $TBAPF_6$, glassy carbon working electrode, vs SCE; values calculated as an average of the cathodic and anodic peaks. [b] ΔE_p= 100 mV.

The cyclic voltammetry of the Rh(III) model compound shows a reduction wave in the 0.0 to −1.0 V cathodic region. The poorly reversible character of this process, assigned to reduction of the Rh(III) center, is as expected on the basis of the general redox behavior of rhodium(III) polypyridine complexes.[38]

The redox behavior of the **Ru−ph$_n$−Rh** dyads (Table 1) is straightforward, by comparison with the model compounds. In the anodic region, the oxidation of the Ru(II) center occurs practically at the same potential for all of the dyads studied, regardless of the number of phenylene spacers. This suggests a weak metal−metal interaction, even through the shortest

(37) The spectrum of **Ru−ph$_3$−Rh** is different from those of the other dyads in the UV region because of the presence on the Ru(II) center of Me_2bpy instead of Me_2phen ligands.

(38) Kalyanasundaram, K. *Photochemistry of Polypyridine and Porphyrin Complexes*; Academic Press: New York, 1992.

Table 2. Luminescence Data of the Model Complexes[a]

	298 K		77 K[b]	
complex	λ_{max} (nm)	τ[c] (μs)	λ_{max} (nm)	τ (ms)
Rh−ph−bpy			495	40
Rh−ph$_2$−bpy			520	42
Rh−ph$_3$′−bpy			495	
$[Rh(Me_2bpy)_3]^{3+}$			450	
Ru−ph−bpy	642	1.5	600	0.007
Ru−ph$_2$−bpy	642	1.5	600	0.006
$[Ru(Me_2phen)_3]^{2+}$	612	1.7	575	0.007
Ru−ph$_3$−bpy	652	1.6	610	0.006
$[Ru(Me_2bpy)_3]^{2+}$	610	1.2	575	0.006

[a] CH_3CN solution. [b] In a 4/1 EtOH/MeOH matrix. [c] Deaerated solution.

Table 3. Photophysical Data of the Dyads[a]

	luminescence					
	298 K		77 K[c]			
dyad	λ_{max} (nm)	τ_{em} (ns)	λ_{max} (nm)	τ_{em} (μs)	transient absorption τ_{abs} (ns)	k_{el}[b] (s^{-1})
Ru−ph−Rh	640	0.360	600	6.9	0.300[d]	3.0×10^9
Ru−ph$_2$−Rh	644	2.3	603	6.8	∼2[d]	4.3×10^8 [e]
Ru−ph$_3$−Rh	652	94[f]	615	6.8	95[f,g]	1.0×10^7
Ru−ph$_3$′−Rh	640	560[f]	600	6.8	540[f,g]	1.1×10^6

[a] Room-temperature CH_3CN solution, unless otherwise noted. [b] Electron-transfer rate constants calculated according to eq 3 (see text), where $\tau = (\tau_{em} + \tau_{abs})/2$ unless otherwise noted. [c] In a 4/1 EtOH/MeOH matrix. [d] Measured at 650 nm. [e] Obtained from emission data. [f] In a deaerated solution. [g] Measured at 460 nm.

bridge. In the cathodic region, the first reduction observed at ca. −0.8 V corresponds for all of the dyads to the reduction of the Rh(III) center. Given the poorly reversible character of the process, the small differences between the various dyads are not considered to be meaningful. The two subsequent reduction waves fall in the same range of potentials as those for the reduction of the polypyridine ligands coordinated to the Ru(II) center, and analogously to the case of the Ru model, the expectation is that the first of this process should involve the bridging ligand.

Photophysical Behavior. (a) Emission Measurements. The emission spectra of all of the complexes were recorded in acetonitrile at room temperature and in 4/1 EtOH/MeOH glass at 77 K. The emission properties of the Ru(II) and Rh(III) model complexes are reported in Table 2.

The Ru(II) model complexes exhibit at room temperature the long-lived MLCT emission typical of the ruthenium(II) polypyridine family. Within the series, the emission properties are very similar (Table 2). The emission maximum is definitely red-shifted with respect to that of $Ru(Me_2phen)_3^{2+}$ or $Ru(Me_2bpy)_3^{2+}$, indicating that in these heteroleptic complexes the lowest emitting triplet involves the MLCT to bpy−ph$_n$−bpy ligand. Differences between systems with different numbers of spacers are negligible, suggesting little delocalization along the ligand in the emitting MLCT triplet.

At 77 K, all of the complexes exhibit a structured MLCT emission with a maximum centered around 600 nm, red-shifted relative to the homoleptic complexes as in the case of the room-temperature emission.

As is generally expected for rhodium(III) polypyridine complexes, the Rh model complexes do not emit at room temperature but show at 77 K the typical, highly structured, LC phosphorescence. The maximum of the high-energy band (Table 2) is shifted to the red with respect to the $Rh(Me_2bpy)_3^{3+}$ homoleptic complex, and the shift increases for the first two terms with the number of phenyl units. This confirms that, in the heteroleptic species, the lowest LC state is on the bpy−ph$_n$−bpy ligand and that in this state the excitation is appreciably delocalized over the whole ligand. Interestingly, for the complex with bpy−ph$_3$′−bpy, the emission maximum occurs at the same energy as that for the complex with the bpy−ph−bpy ligand, indicating that the alkyl chains are effective in decreasing the electronic delocalization.

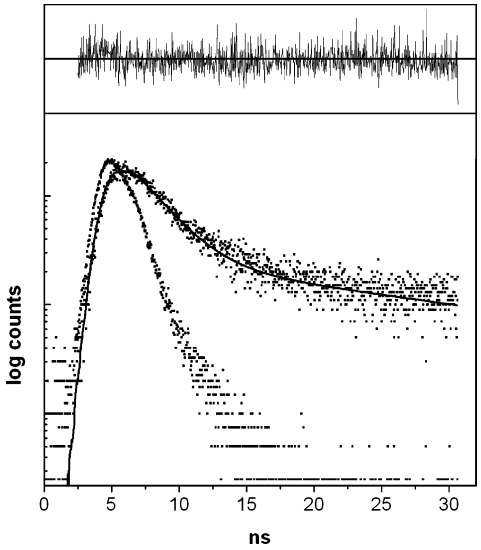

Figure 2. Experimental emission decay (with a superimposed lamp profile) of **Ru−ph$_2$−Rh** obtained by time-correlated single-photon counting in a room-temperature acetonitrile solution. The solid line represents the fit of the data points to a two-exponential decay law with lifetimes of 2.1 ns (93%) and 50 ns (7%); see text.

As far as the photophysical behavior of the dyads is concerned (Table 3), the important result is that at room temperature the typical MLCT emission of this unit is always quenched with respect to that of the Ru(II) models. Spectrofluorimetric experiments performed on absorbance-matched solutions of the dyads and the appropriate Ru(II) model compounds indicated that the extent of quenching decreases with the increasing number of phenyl units of the bridging ligand ($n = 1-3$). A significant observation is that the extent of quenching is significantly smaller for **Ru−ph$_3$′−Rh** with respect to **Ru−ph$_3$−Rh**. For all of the dyads, the maximum of the residual Ru(II)-based emission (Table 3) is practically identical with that of the Ru(II) model (Table 2).

The emission lifetimes were measured in a deaerated CH_3CN solution by different techniques depending on the time scale of the experimental decays. For **Ru−ph$_3$′−Rh**, **Ru−ph$_3$−Rh**, and **Ru−ph$_2$−Rh**, single-photon-counting experiments were performed. The observed decay for **Ru−ph$_2$−Rh** is presented in Figure 2 as an example.

In the case of the **Ru−ph−Rh** dyad, the decay of the emission was measured by picosecond time-resolved emission spectroscopy (see the Experimental Section). For all of

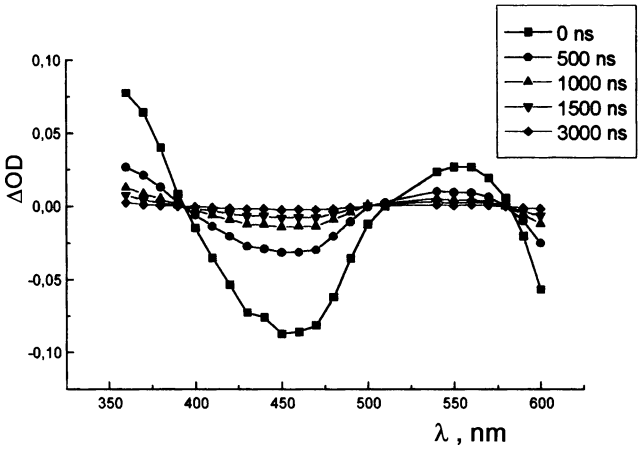

Figure 3. Time-resolved transient absorption spectrum of **Ru−ph$_3$′−Rh** in a deaerated acetonitrile solution recorded at different delay times after excitation (λ_{exc} = 532 nm).

the dyads studied, the emission decay was not strictly monoexponential, involving, besides a major (85−95%) component, also a minor (15−5%) tail of longer (ca. 1 order of magnitude) lifetime than the main first component. The values of the lifetime of the main component (Table 3) are always remarkably short-lived with respect to those of the Ru(II) model complexes (Table 2). Interestingly, the values are strongly dependent on the length of the bridge, increasing gradually with the number of phenyl units in the order **Ru−ph−Rh** < **Ru−ph$_2$−Rh** < **Ru−ph$_3$−Rh** < **Ru−ph$_3$′−Rh**. Again, within the series, the dyad with the phenyl unit bearing hexyl chains appears to have very different behavior (a much longer lifetime) than its simple analogue.

The emission properties of **Ru−ph$_n$−Rh** dyads were also studied in a rigid matrix at 77 K (4/1 EtOH/MeOH). Under these conditions, a very similar behavior is observed for all systems investigated: the Ru(II)-based emission is not quenched, the emission decay is monoexponential with a lifetime practically identical with that of a Ru(II)-free model complex (7 μs).

(b) Transient Absorption Measurements. The **Ru−ph$_3$′−Rh** and **Ru−ph$_3$−Rh** dyads were investigated by conventional (nanosecond) laser flash photolysis, while for **Ru−ph−Rh** and **Ru−ph$_2$−Rh** ultrafast (femtosecond) spectroscopy experiments were required.

The transient absorption spectrum of **Ru−ph$_3$′−Rh** obtained immediately following laser excitation at 532 nm, where light is selectively absorbed by the Ru(II) molecular component, is depicted in Figure 3.

The transient changes consist of a positive absorption at ca. 360 nm and a strong bleaching centered at 460 nm. The apparent bleaching observed at λ > 550 nm is actually due to light emission from the sample. This difference spectrum, virtually identical with those obtained with the mononuclear models, is typical of the formation of the triplet MLCT excited state of a Ru(II)-based component. In Figure 3 are also reported the time-resolved spectral changes obtained for **Ru−ph$_3$′−Rh** at different delay times after the laser pulse. The transient changes decay to the original baseline, with a constant spectral profile and with isosbestic points at 395 and 505 nm. These observations suggest that the conversion of the initially formed MLCT state to the ground state occurs without intermediate formation of other products. The same qualitative time-resolved absorption behavior, with clean spectral changes and isosbestic points, is also observed for the **Ru−ph$_3$−Rh** dyad. For the two dyads, however, the spectral changes decay in remarkably different times scales: microseconds for **Ru−ph$_3$′−Rh** and hundreds of nanoseconds for **Ru−ph$_3$−Rh**. The decay kinetics (measured at 450 nm; recovery of ground-state absorption bleaching) are compared in Figure 4.

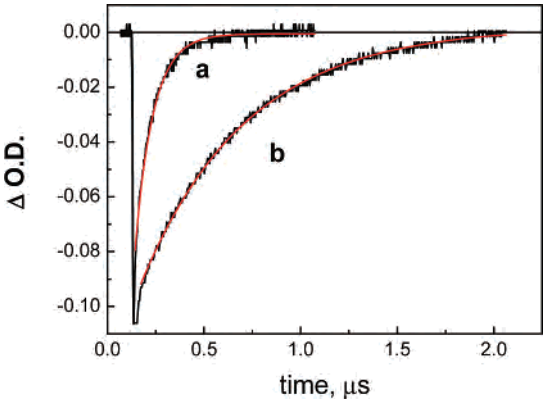

Figure 4. Kinetic profiles at 460 nm following excitation of **Ru−ph$_3$−Rh** (a) and **Ru−ph$_3$′−Rh** (b) in a deaerated acetonitrile solution at room temperature with a 8-ns laser pulse at 532 nm. The red lines drawn in the experimental traces represent a fit of the data points to a two-exponential law with lifetimes of 90 ns (95%) and 1000 ns (5%) for trace a and of 450 ns (90%) and 1500 ns (10%) for trace b.

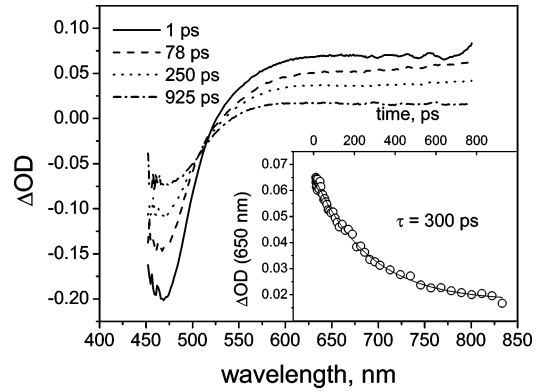

Figure 5. Transient spectral changes measured in ultrafast spectroscopy for **Ru−ph−Rh** in an acetonitrile solution. Inset: kinetic trace monitored at 650 nm. The solid line represents a fit of the data points to a single-exponential decay law.

The decay profiles are independent of the wavelength and fit reasonably well to a two-exponential decay law (main component plus a minor long-lived tail) similar to that observed in emission. The lifetimes of the main component are reported in Table 3.

The transient behavior observed following 400-nm excitation of CH_3CN solutions of **Ru−ph−Rh** in ultrafast measurements is summarized in Figure 5. The transient spectrum is characterized by ground-state bleaching around 460 nm and a wide absorption at λ > 550 nm corresponding to the formation of a MLCT triplet state of the Ru(II) component. The kinetic profile of the absorption at 650 nm fits reasonably well to a single-exponential decay law with a lifetime of

270 ps (Table 3). As observed for the other dyads, a minor component with a longer (nanosecond) lifetime is revealed by the residual differential absorption at the end of the experiment in Figure 5.

A very similar initial transient spectrum was obtained in the ultrafast spectroscopy of the **Ru−ph$_2$−Rh** dyad. In this case, the kinetics was slower and only a relatively small portion of the decay could be observed within the 1-ns time window of the experiment. Analysis of the decay at 650 nm yields an approximate lifetime of 1.6 ns (Table 3).

Discussion

Properties of Molecular Components and Energy Levels of the Dyads. The absorption spectra of the dyads (Figure 1) are practically the superposition of the spectra of the isolated mononuclear model complexes. In the UV region, where overlapping LC bands of both Ru(II) and Rh(III) molecular components are present, the spectra change dramatically with the number and nature of phenylene units. In particular, the absorption in the 320−400-nm region increases and shifts slightly to lower energy by changing the spacer, for the Ru(II)−Rh(III) dyads as well as for the Ru(II) and Rh(III) mononuclear models. This behavior, typical of oligophenylenes,[39] clearly indicates that the LC excited states of the bpy−ph$_n$−bpy ligand are at least partially delocalized over the phenylene chain. The observed change in the spectral shifts (in the order $n = 1, 3', 2, 3$) indicates that the extent of LC delocalization depends not only on the number of phenylene units but also on the presence of substituents on the phenyl ring. In particular, in the **Ru−ph$_3$′−Rh** dyad, the bridge absorption is much weaker and blue-shifted with respect to the unsubstituted analogue **Ru−ph$_3$−Rh**. This can be easily explained considering the effect of substitution on the dihedral angle between adjacent phenylene spacers. This angle, which in the ground state of unsubstituted systems is ca. 40°, is expected to increase substantially as a consequence of increased steric hindrance upon alkyl substitution. This is expected to reduce strongly the delocalization of the LC state along the oligophenylene chain, thus justifying the "anomalous" spectroscopic behavior of the $n = 3'$ system. In the visible region spectra, on the other hand, the dyads are characterized by the typical MLCT transitions of the Ru(II) component (Figure 1). In the lowest MLCT excited state, the excited electron is most probably localized on the bridging ligand rather than on the terminal ones.[24] The appreciable independence of the MLCT band energy and intensity on the number/nature of phenylene spacers seems to indicate that, in contrast to what happens for LC states, the extent of delocalization of the MLCT states onto the phenylene chain is modest.

Excitation of the dyads at 532 nm (flash photolysis experiments) or 400 nm (ultrafast spectroscopy) leads to selective or predominant, respectively, MLCT excitation. A simplified energy level diagram suitable for the discussion of the photophysical behavior of the dyads under these conditions is shown in Figure 6. This diagram holds for the whole series of **Ru−ph$_n$−Rh** dyads, with minor quantitative differences with changes of the number of phenyl units. The excited states represented are the lowest MLCT excited states of the Ru(II) unit (quantitatively in subpicosecond time from upper spectroscopic states) and an intercomponent electron-transfer state of Ru(III)−Rh(II) character. As usual, the energy of the MLCT triplet state, 2.05 eV, is estimated from the 77 K emission data of the dyads (Table 3). The energy of the intercomponent charge-transfer state, ca. 2.00 eV, can be obtained from electrochemical data of the dyads (Table 1) as the difference in the potentials for oxidation of Ru(II) and for reduction of Rh(III). No correction for electrostatic work terms is required in this case because of the charge shift character [*Ru(II)−Rh(III) → Ru(III)−Rh(II)] of the process involved. When the small differences between the various dyads are disregarded, an average value of ca. 2.00 ± 0.03 eV is obtained from the data in Table 1 for the energy of the charge-transfer state. The conclusion is that in the whole series of dyads the local MLCT excited state *Ru(II)−Rh(III) and the Ru(III)−Rh(II) electron-transfer state are very close in energy, with a small estimated average driving force for electron-transfer quenching of ca. 50 meV.

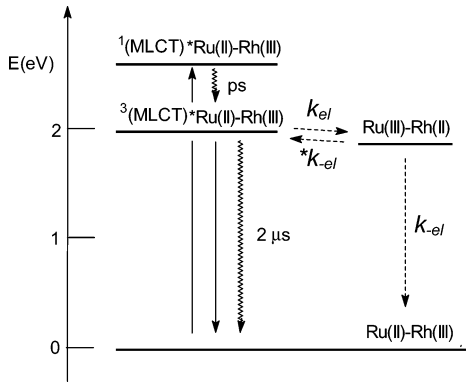

Figure 6. Energy level diagram for **Ru−ph$_n$−Rh** dyads.

In the diagram (Figure 6) are indicated the common photophysical processes taking place within the Ru(II) component, i.e., prompt (<1 ps) intersystem crossing to form the long-lived triplet MLCT state, followed by radiative and radiationless deactivation (which in mononuclear models take place in ca. 1.5 μs). Also indicated are a number of plausible intercomponent processes, including (i) electron transfer from excited Ru(II) to Rh(III), (ii) back electron transfer to reform the Ru(II)-based MLCT excited state, and (iii) back electron transfer to the ground state of the dyad.

Photoinduced Electron Transfer. The important photophysical results can be summarized as follows.

The Ru(II)-based emission has a much smaller intensity and a faster decay with respect to the corresponding Ru(II) mononuclear model, clearly indicating that efficient intramolecular quenching of the Ru(II)-based MLCT state takes places. On the basis of the energy level diagram (Figure 6), the likely pathway for the observed quenching is photoinduced intramolecular electron transfer.

In time-resolved absorption spectroscopy, the Ru(II)-based MLCT state seems to decay to the ground state without

(39) Zojer, E.; Cornil, J.; Leising, G.; Brédas, J. L. *Phys. Rev. B* **1999**, *59*, 7957.

appreciable accumulation of the charge-separated products. The kinetics generally parallel those observed in emission.

The decay kinetics, in both emission and absorption, are always nonexponential, involving, besides a major component of shorter lifetime, a minor (5−15%) component of longer lifetime.

In principle, various explanations could be given for the complex decay behavior.

One possibility is that reversible excited-state electron transfer can lead to equilibration between the (^{3}MLCT)*Ru(II)−Rh(III) state and the Ru(III)−Rh(II) "charge-separated" state, prior to charge recombination to the ground state (eq 2; $k_{el} > {}^*k_{-el} \gg k_{-el}$). In this case, the fast decay could be associated with relaxation of the MLCT toward equilibrium and the slow one with the decay of the two states in equilibrium with the ground state. It should be remarked, however, that the ratio between the fast and slow components, as well as the negligible formation of the charge-separated state observed in time-resolved spectroscopy, would require that excited-state equilibrium be strongly displaced toward the MLCT state. This is very unlikely, given the known energetics of the systems (Figure 6).

$$(^3\text{MLCT})^*\text{Ru(II)}-\text{Rh(III)} \underset{{}^*k_{-el}}{\overset{k_{el}}{\rightleftharpoons}} \text{Ru(III)}-\text{Rh(II)} \xrightarrow{k_{-el}} \text{Ru(II)}-\text{Rh(III)} \quad (2)$$

The alternative explanation relies on a kinetic scheme in which charge separation is followed by fast charge recombination (eq 2; $k_{el} \ll k_{-el} \gg {}^*k_{-el}$). This explains obviously the negligible accumulation of charge-separated products. In this case, the biexponential decay could be associated with the presence of different conformers of the dyads in solution, with different electron-transfer kinetics. In dyads of this type, conformational flexibility may be associated either with the double-well torsional potential[40] governing the twist angles in the oligophenylene spacer or with torsional degrees of freedom at the linkages between the bridge and the donor or acceptor units. Conformational effects in dyads with oligophenylene bridges have been recently documented.[22c]

In conclusion, the experimental data strongly suggest that the decay of the Ru(II)−Rh(III) excited state leads to the ground state via a sequence of forward (k_{el}, rate determining) and back (k_{-el}, fast) electron-transfer steps, without any appreciable accumulation of the Ru(II)−Rh(III) charge-separated state. The biphasic behavior is attributed to conformational effects. These features seem to be common to ruthenium(II)−rhodium(III) polypyridine dyads.[26,31] In the following discussion, the major component of the decay, as obtained from either the emission or time-resolved absorption data (Table 3), will be used in the calculation of the photoinduced electron-transfer rate constants with eq 3,

$$k_{el} = 1/\tau - 1/\tau^0 \quad (3)$$

where τ and τ^0 are the lifetimes of the MLCT state in the dyad and in the appropriate mononuclear model. The values of k_{el} for the whole series of dyads are reported in Table 3.

For all dyads at 77 K, no quenching of the typical MLCT Ru-based emission takes place (see Table 3), clearly indicating that the electron-transfer process does not occur under these experimental conditions. This behavior is in line with what is expected to occur for processes that are slightly exergonic in fluid solution.[26,31]

Bridge and Distance Effects. The rate constants for the photoinduced electron-transfer process reported in Table 3 indicate, as expected, a decrease of the electron-transfer rates with an increase in the bridge length. This trend can be analyzed in terms of standard electron-transfer theory. Given the negligible intercomponent perturbation observed (additivity of the spectroscopic and electrochemical properties of the metal-based molecular components), we assume that the intercomponent electronic coupling is sufficiently small that the electron-transfer reactions belong to the weak-interaction (nonadiabatic) regime. In this limit, the rate constant is given by[16]

$$k_{el} = \frac{2\pi}{\hbar} H_{AB}{}^2(\text{FCWD}) \quad (4)$$

where H_{AB} is the electronic coupling matrix element and FCWD is the nuclear term (Franck−Condon weighted density of states), which accounts for the combined effects of the reorganizational energies and driving force. In principle, both terms are distance-dependent, but by far the strongest dependence is expected to lie in the electronic factor. In the frame of the superexchange mechanism, H_{AB} follows an exponential decay with the distance given by the expression

$$H_{AB}{}^2 = H_{AB}{}^2(0) \exp[-\beta(r)] \quad (5)$$

where r is the donor−acceptor distance, $H_{AB}(0)$ is the hypothetical interaction at the contact distance, and β is an appropriate attenuation parameter. Thus, if the distance dependence of the nuclear factor can be neglected, also the rate constant should fall off exponentially with the distance, as in eq 1.

The experimental rate constants for all of the dyads studied are displayed on a logarithmic plot as a function of the donor−acceptor distance in Figure 7. It can be seen that the three systems with unsubstituted polyphenylene spacers exhibit a clear exponential dependence of the rates on distance. This is the behavior predicted by eq 1 and is thus consistent with a superexchange (through-bond) mechanism. From the slope of the line in Figure 7, an attenuation factor β (eq 1) of 0.65 Å^{-1} can be determined. It is important to recall that this value is obtained by neglecting the distance dependence of the FCWD term. This assumption is an oversimplification that deserves further discussion. In general, the FCWD term may exhibit some distance dependence through (a) the solvent reorganizational energy and (b) the driving force. For the Ru(II)−Rh(III) dyads, however, given the charge-shift nature of the process, the driving force is

(40) (a) Zhuravlev, K. K.; McCluskey, M. D. *J. Chem. Phys.* **2004**, *120*, 1841. (b) Heimel, G.; Daghofer, M.; Gierschner, J.; List, E. J. W.; Grimsdale, A. C.; Mullen, K.; Belijonne, D.; Bredas, J.-L.; Zojer, E. *J. Chem. Phys.* **2005**, *122*, 054501.

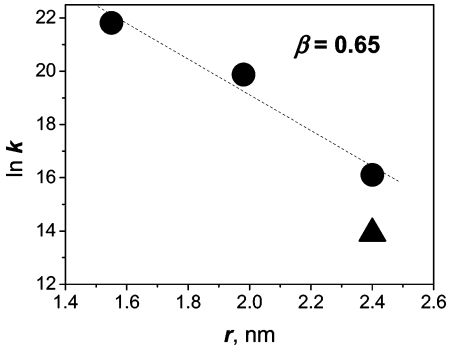

Figure 7. Plot of ln k_{el} vs the metal−metal distance for dyads **Ru−ph$_n$−Rh** with bare phenylene units (circles) and for **Ru−ph$_3$′−Rh** with *n*-hexyl chains on the central phenylene unit (triangle).

independent of the donor−acceptor distance. The solvent reorganizational energy, on the other hand, is expected to increase slightly with the distance according to standard models.[16]

Its contribution to the observed rate decrease is presumably relatively small, but it is difficult to evaluate exactly its dependence on the assumed weight of this term in the total reorganizational energy. Therefore, the β value obtained from the slope of the line in Figure 7, 0.65 Å^{-1}, should be regarded as an upper limiting value for the attenuation factor of the intercomponent electronic coupling (eq 1).

From a general viewpoint, the attenuation factor obtained in this study lies in a typical range for oligophenylene bridges. This value can be compared to that reported for photoinduced electron transfer across *p*-oligophenylene spacers between porphyrins by McLendon and co-workers[21] (0.4 Å^{-1}) and more recently by Wasielewski and co-workers[22a] for organic donor−acceptor systems (0.46−0.67 Å^{-1}). Interestingly, similar attenuation factor values (0.61 Å^{-1}) were obtained by measuring electron-transfer rates across oligophenylene spacers in metal−molecules−metal junctions.[10b,41] Such β values are lower than those for rigid aliphatic bridges (typical values of 0.8−1.2 Å^{-1}) and underline the good ability of the oligophenylene bridges to mediate donor−acceptor electronic coupling. In this regard, it is instructive to compare the electron-transfer rate constant observed for **Ru−ph−Rh** ($k = 3.0 \times 10^9$ s^{-1}) with that previously measured[31] for the dyad **Ru−(CH$_2$)$_2$−Rh** ($k = 1.7 \times 10^8$ s^{-1}).

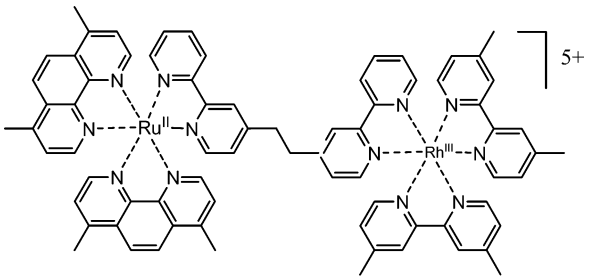

Ru-(CH$_2$)$_2$-Rh

These two systems have the same donor and acceptor units connected by different bridges. Despite the longer metal−metal distance (15.5 Å for **Ru−ph−Rh** relative to 13.5 Å for **Ru−(CH$_2$)−Rh**), the reaction is faster across the phenylene spacer by more than 1 order of magnitude.

An important observation made in this study is worthy of comment. It can be clearly seen from Figure 7 that the rate constant for dyad **Ru−ph$_3$′−Rh** does not fall on the linear plot obtained for the other dyads. In fact, dyad **Ru−ph$_3$′−Rh**, which is identical with **Ru−ph$_3$−Rh** except for the presence of two solubilizing hexyl groups on the central phenylene ring, undergoes photoinduced electron transfer 10 times slower than its unsubstituted analogue. The reason of this behavior is most likely related to the notion that, in a superexchange mechanism with modular spacer, the rate is sensitive to the electronic couplings between adjacent modules[5,28] and with oligophenylene bridges this coupling is a sensitive function of the twist angle between adjacent modules.[42] Substitution at the central phenylene rings causes increased steric hindrance, and thus increased twist angle with the adjacent units. The consequence is a decrease in the local electronic couplings that translates into a decrease in the overall superexchange coupling and into a drastic slowing down of the electron-transfer process. Analogous effects of substitution have been recently reported for Dexter energy-transfer processes in Ru(II)−Os(II) dyads with oligophenylene bridges.[24c]

Conclusion

The study of the Ru(II)−Rh(III) dyads has confirmed that rigid oligophenylene bridges are efficient mediators of long-distance photoinduced electron transfer between transition-metal polypyridine units. In the longer system studied, dyad **Ru−ph$_3$−Rh**, photoinduced electron transfer is still 70% efficient over a distance of 24 Å. The sharp difference in the rates observed between identical dyads differing only in the presence of alkyl substituents in the central *p*-phenylene ring highlights the importance of the bridge conformation on the overall through-bond donor−acceptor coupling. The dependence of the electronic coupling on the intermodule twist angle can be used for synthetic tuning.[24c,43,44] If some kind of external control could be achieved on the inter-ring angles, these effects could also be used, in principle, for switching purposes.

Acknowledgment. We thank Dr. A. Prodi for electrochemical measurements and Prof. Russel H. Schmehl (Tulane University) for supplying us with samples of bpy−ph−bpy and bpy−ph$_2$−bpy. Financial support from EC (Grant G5RD-CT-2002-00776, MWFM) and MIUR (Grant FIRB-RBNE019H9K) is gratefully acknowledged.

Supporting Information Available: ^{1}H NMR spectra, cyclic voltammograms, and ESI-MS spectra. This material is available free of charge via the Internet at http://pubs.acs.org.

IC700430U

(41) Wold, D. J.; Haag, R.; Rampi, M. A.; Frisbie, C. D. *J. Phys. Chem. B* **2002**, *106*, 2814.
(42) Toutounji, M. M.; Ratner, M. A. *J. Phys. Chem. A* **2000**, *104*, 8566.
(43) Benniston, A. C.; Harriman, A.; Li, P.; Sams, C. A.; Ward, M. D. *J. Am. Chem. Soc.* **2004**, *126*, 13630.
(44) Lainé, F. P.; Bedioui, F.; Loiseau, F.; Chiorboli, C.; Campagna, S. *J. Am. Chem. Soc.* **2006**, *128*, 7510.